ELSEVIER

Journal of Power Sources 54 (1995) 109–114

JOURNAL OF POWER SOURCES

Li_xNiO_2, a promising cathode for rechargeable lithium batteries

M. Broussely [a], F. Perton [a], P. Biensan [a], J.M. Bodet [a], J. Labat [a], A. Lecerf [b], C. Delmas [c], A. Rougier [c], J.P. Pérès [c]

[a] *SAFT Advanced Battery Division, BP 1039, 86060 Poitiers, France*

[b] *INSA, 20 avenue des Buttes de Coësmes, 35043 Rennes, France*

[c] *Laboratoire de Chimie du Solide du CNRS, and Ecole Nationale Supérieure de Chimie et Physique de Bordeaux, 351 cours de la Libération, 33405 Talence, France*

Abstract

Lithiated nickel oxide has been prepared and studied with the aim of using it as the positive active reversible material in rechargeable lithium batteries. This paper describes the particular features of this material, and discusses the results that demonstrate its interest as cathode in practical cells, using carbon as the negative electrode. Specific energy and energy density of more than 130 Wh/kg and 320 Wh/l were obtained in prototypes, and a cycleability of over 1000 cycles was demonstrated.

Keywords: Rechargeable lithium batteries; Lithiated nickel oxide; Nickel oxide

1. Introduction

The recent development of the 'Li-ion' concept for rechargeable lithium batteries, required the use of prelithiated compounds, to allow the use of carbonaceous materials as the negative reversible electrode. Few materials are, up to now, able to give at the same time: high energy, high reversibility, and low cost. Lithiated nickel oxide, $LiNiO_2$, is one of these compounds, competing with $LiCoO_2$ and Li_xMnO_2. The main advantages of $LiNiO_2$ are the lower cost compared with $LiCoO_2$, and the better electrochemical performances compared with those of $LiCoO_2$ and Li_xMnO_2. Manganese lithiated oxide remains attractive for cost and environmental issues providing that a sufficient practical energy density can be achieved. One of the reasons why $LiCoO_2$ is, up to now, more widely used in the industry despite its price, is that its synthesis on industrial scale is easier. This, however, can also be achieved for $LiNiO_2$, using $LiOH \cdot H_2O$ as lithiating agent, as described in Ref. [1]. The material so obtained has a very good electrochemical activity.

2. Material synthesis and crystalline structure

The synthesis of $LiNiO_2$ has already been described [1,2]. It consists of heating a mixture of $LiOH \cdot H_2O$ and NiO powders, in the appropriate ratio, at up to about 700 °C in air, during a period of time depending on the furnace characteristics and amount treated. The resulting compound obtained after grinding has the general formula $Li_{1-z}Ni_{1+z}O_2$, in which z is close to 0, and oxidation degree of Ni > 2.95. A semi-industrial process has been set up to produce quantities of 200 kg per batch.

Lithium nickel oxide has been characterized by X-ray diffraction (XRD) which shows that this material is very well crystallized (Fig. 1). For the $LiNiO_2$ stoi-

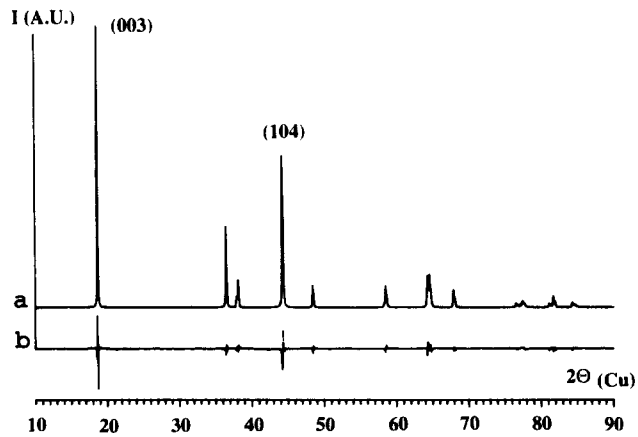

Fig. 1. (a) X-ray diffraction profile of '$LiNiO_2$' (0.02(2θ), 40 s scans). (b) Profile of the intensity difference between experimental and calculated X-ray diffraction patterns.

SSDI 0378-7753(94)02049-9

chiometric composition, Li^+ and Ni^{3+} ions occupy the octahedral sites of f.c.c. oxygen anions packing; these cations are ordered along the [111] direction of the rocksalt cubic lattice, leading to a 2D structure. In fact, as previously mentioned, the general formula of this materials family is $Li_{1-z}Ni_{1+z}O_2$ with extra-nickel ions located in the interslab space of this layered structure (i.e., within the lithium site). This phase crystallizes in the rhombohedral system (SG: $R\bar{3}m$); the hexagonal parameters are $a = 2.8806_1$ Å and $c = 14.2050_5$ Å. The value of the c/a ratio (equal to 4.93) is slightly different from $2\sqrt{6}$ (characteristic of a cubic lattice). This departure results from the strong structural anisotropy related to the 2D structure. The X-ray pattern of this material has been studied by Rietveld refinement; the best fit has been obtained for a value of z equal to 0.03 as evidenced by the low R values ($R_{Bragg} = 2.40\%$, $R_F = 2.47\%$, $R_{wp} = 7.46\%$). The good agreement between the experimental and the calculated pattern is emphasized by the difference pattern also reported in Fig. 1. This very small value of z must be compared with those generally reported for lithium nickel oxide for which z varies in the 0.05–0.20 range. Therefore, the corresponding formula ($Li_{0.97}Ni_{1.03}O_2$) is very close to the ideal one, as it was primarily suggested by the intensity ratio of the (003) and the (104) X-ray diffraction lines [3]; moreover, it is very close to this recently reported by Rougier et al. [4] who have obtained a 2D $LiNiO_2$. This result shows that the involved preparation method leads to a quasi-2D material which must be therefore particularly well adapted to the lithium de-intercalation and intercalation.

3. Electrochemical characteristics

Some electrochemical properties of $LiNiO_2$ have been given in Refs. [2,5], and the relation between the electrochemical behaviour and the crystalline structure has been described in Refs. [6–9]. The difficulty is that this material can be prepared in different ways which do not lead to similar compositions [6]. It is well admitted that a slight difference in stoichiometry induces significant variations in the electrochemical properties. This can be attributed to the presence of nickel ions in the lithium layers, as described above.

3.1. Voltage profile

The voltage profile, studied at low rate, exhibits different domains of electrochemical lithium insertion, in good accordance with already published results. These experiments were made using a thin electrode containing 88.3% of active material, blended with 10.5% mixture of graphite and acetylene black (A.B.) as conductive agent, and 1.2% of polytetrafluoroethylene binder. Each electrode contains about 34 mg of this mixture. Fig. 2(a) shows the first cycles obtained at 0.3 mA, corresponding to an approximately 30 h rate, based on 1 Li/mol. The electrolyte consisted of 1 M $LiClO_4$ in propylene carbonate.

The differential curve $-dx/|dV| = f(V)$ (Fig. 2(b)) shows more clearly the different steps attributed to several phases [6,7], which are under further investigation. The working discharge voltage range of this oxide is thus from about 3 to 4 V, close to $LiCoO_2$. Its unique feature is the possibility, within a voltage range slightly lower than $LiCoO_2$, up to 4.1 V versus Li, to produce about 0.65 Li^+/mol during the first charge (175 Ah/kg) at a constant rate of $C/5$. A higher voltage charge (4.2 V), or lower rate, or taper constant voltage end of charge, results in a higher capacity, up to 200 Ah/kg, corresponding to $Li_{0.26}NiO_2$. However, this initial amount of extracted lithium is not reversibly

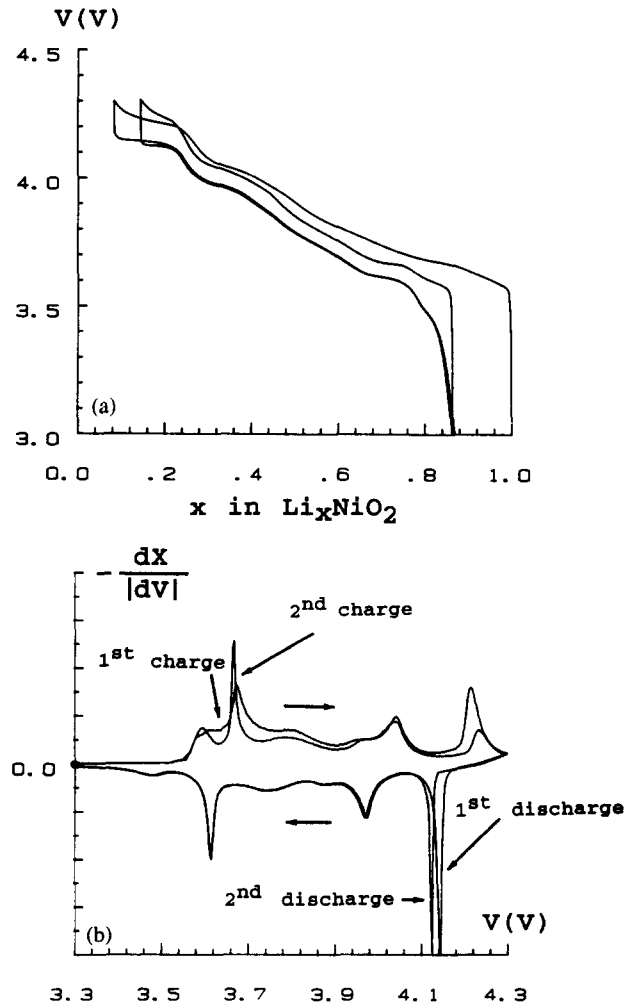

Fig. 2. Charge/discharge characteristics of Li/Li_xNiO_2 in 1 M $LiClO_4$/propylene carbonate at $I = 300$ μA, and $V_{max} = 4.35$ V. (a) Voltage variation vs. x. (b) Differential curve $-dx/|dV|$ vs. x.

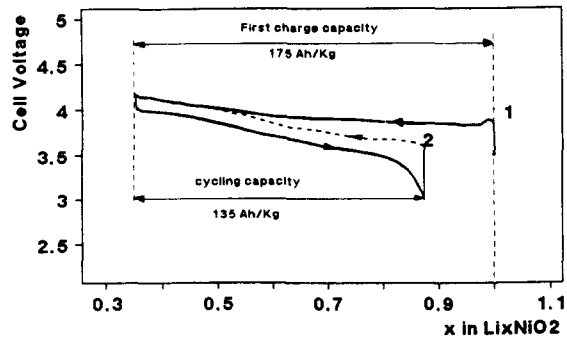

Fig. 3. Typical first cycle behaviour of Li/Li_xNiO_2 system at *C*/5 rate.

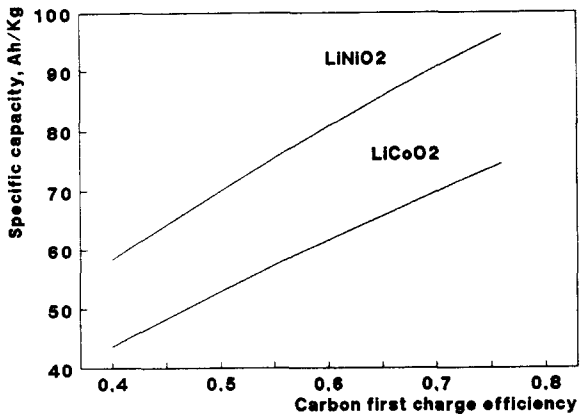

Fig. 4. Calculated specific capacity of whole active balanced materials in function of carbon efficiency at first cycle, reversible capacity of carbon = 345 Ah/kg.

re-inserted (Fig. 3), and a material having the composition $Li_{0.85}NiO_2$ is obtained as end-discharge product. This new composition is nevertheless fully reversible on subsequent charge/discharge cycles. In fact, the reversible reaction can be described as:

$$Li_{0.35}NiO_2 + 0.5Li^+ + 0.5e^- \longleftrightarrow Li_{0.85}NiO_2 \quad (1)$$

when cycled at a constant medium/high rate (*C*/5 to *C*) within the voltage range from 4.1 to 2.7 V. This excess of lithium at the first cycle (about 30%, depending on the first charge conditions) is very useful to passivate the negative electrode, which own charge efficiency at the first cycle is in the range from 60 to 80%. Thus, the design of the cell does not need large excess of cathode which limits the energy density. This results in a significative improvement in the specific capacity of the electrochemical components, as shown in Fig. 4. This figure describes a calculated specific capacity of the materials, properly balanced, versus carbon efficiency at the first cycle, using either $LiCoO_2$ (135 Ah/kg reversible to 4.2 V) or $LiNiO_2$ (125 Ah/kg reversible to 4.1 V). The specific reversible capacity of carbon used for that calculation is 345 Ah/kg.

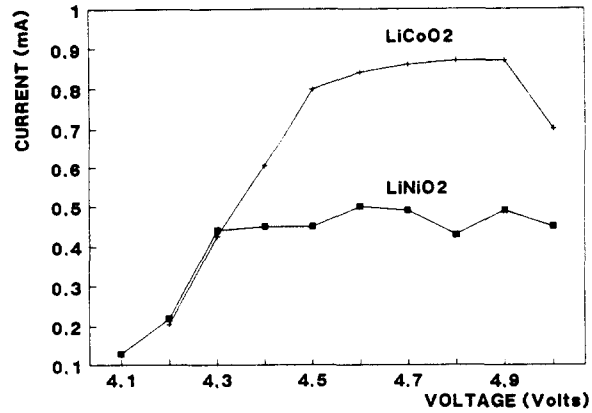

Fig. 5. Comparison of overcharge current in function of voltage for $LiNiO_2$ and $LiCoO_2$. The current is recorded on initially charged electrodes, after 0.5 h rest at constant voltage.

3.2. Overcharge characteristics

Some experiments were performed to compare the electrochemical behaviour of nickel and cobalt lithiated oxides charged at a higher voltage than the specified maxima. Fig. 5 shows the current recorded after 30 min rest at each voltage. Electrodes were initially charged at 4.1 V for $LiNiO_2$, and 4.2 V for $LiCoO_2$. The pseudo steady-state values obtained at 5 V after 15 h were 0.16 and 0.066 mA for $LiCoO_2$ and $LiNiO_2$, respectively. These results were obtained at ambient temperature in flooded cells, using an appropriate electrolyte. As it can be seen, the overcharge current for nickel oxide is always lower than for cobalt oxide.

4. Cell performances

Prototypes of several cylindrical cells were built using the spiral configuration. $LiNiO_2$ was associated to different types of carbon. An appropriate non-aqueous electrolyte and a polypropylene microporous separator were used. Fig. 6 shows typical electrical performances of a 4/5 'A'-size cell (height = 42.4 mm, diameter = 16.6 mm) at low (*C*/5) and high (2*C*) discharge rates. As it can be seen, the working voltage of this cell varies during discharge between 4 and 3 V, which is very close to the voltage exhibited by Li_yC/Li_xCoO_2 system. The sloping voltage can be easily used as state-of-charge indicator. Specific energy and energy density values of 113 Wh/kg and 282 Wh/l, respectively, were so obtained at the *C*/5 rate. A typical charge/discharge cycle at *C*/5 is shown in Fig. 7. The voltage limit for charge was set at 4.1 V, a slightly lower value than for $LiCoO_2$, favourable for electrolyte stability. This figure shows the good energy efficiency of this system. On larger

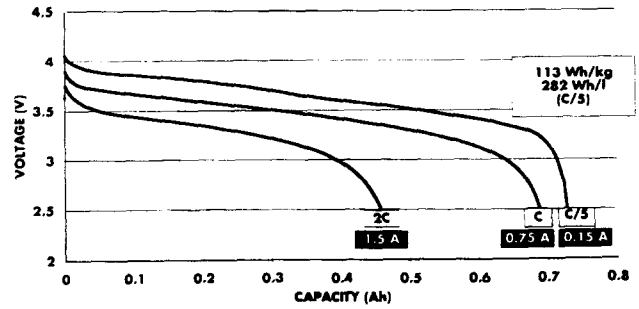

Fig. 6. Discharge curves of 4/5 'A'-size Li_yC/Li_xNiO_2 battery at various rates.

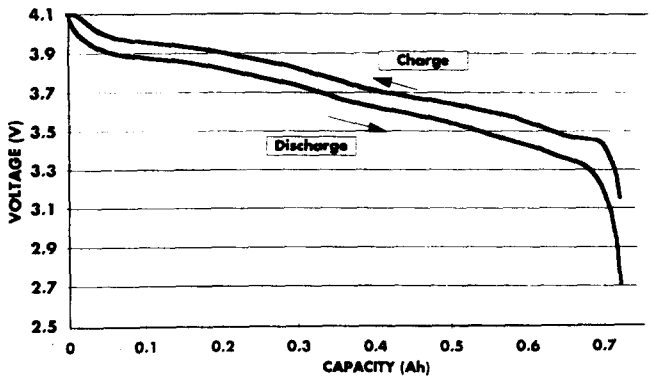

Fig. 7. Charge/discharge profile of a 4/5 'A'-size Li_yC/Li_xNiO_2 battery at a 5 h rate.

'D'-size cells, energy density of 320 Wh/l and specific energy of 130 Wh/kg were demonstrated.

4.1. Cycle life

A long cycle-life test was performed, using a laboratory cell with a slightly smaller size than 'C'. Fig. 8 shows the capacity evolution, during 1200 cycles, at 100% depth-of-discharge, at the *C* rate for charge and discharge. A fairly good capacity stability was obtained, more than 60% of the initial capacity being still available at this rate after 1000 cycles. The discharge of the 800th cycle, still made at the 1 h rate, but after a low rate charge, indicates that the limitation is of kinetic nature, 91% of the initial capacity being recovered. No significant lithium corrosion was therefore occurring, during this 8-month cycling test at room temperature, proving the quite good stability of the protecting layer on carbon. This is confirmed by a cell postmortem analysis at the discharged state, which indicates that the correct amount of lithium corresponding to a complete discharged cathode is still inserted in the cathode. The kinetic effect, which could be due to a change in the cathode mixture morphology, prevents a complete charge once the maximum voltage, including polarization, has been reached.

The positive electrode materials recovered at the end of the 5th, 250th and 1200th discharge of $C/LiNiO_2$

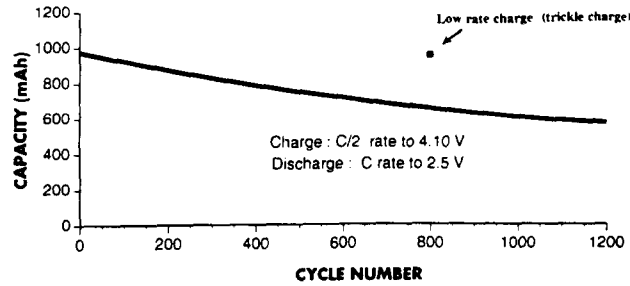

Fig. 8. Evolution of the capacity during cycling of an Li_yC/Li_xNiO_2 battery at ambient temperature; charge = *C*/2 rate to 4.1 V, discharge = *C* rate to 2.5 V.

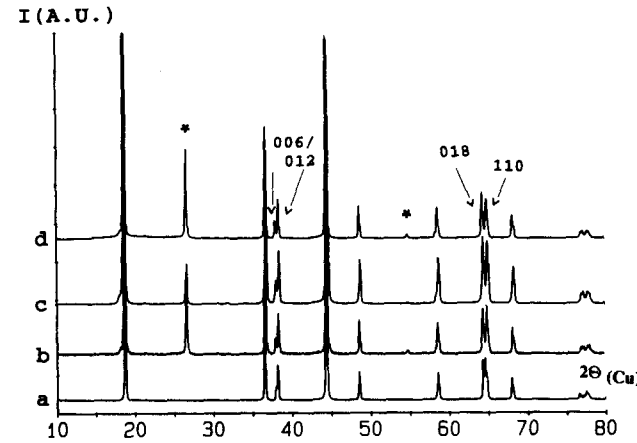

Fig. 9. Comparison between the X-ray diffraction profile (0.02(2θ), 15 s scans) of the $LiNiO_2$ uncycled phase (a) and the X-ray diffraction profiles of the 'Li_xNiO_2' phases recovered at the end of the 5th (b), 250th (c), and 1200th (d) discharge of the $Li_yC/LiNiO_2$ batteries. (* indicates diffraction lines of the carbon added as electronic conductor within the positive electrode.)

batteries have also been studied in order to prove modifications from the structural and textural point of view. Fig. 9 represents the XRD patterns of these materials in comparison with those of the uncycled phase. In all cases, the $LiNiO_2$ structural type is maintained. As emphasized by the splitting of the (006)/(012) and (110)/(018) lines in the XRD patterns, the reticular distances are slightly different for the various materials. Nevertheless, as no structural refinement has still been performed, no conclusion about a possible modification of the nickel distribution within the f.c.c. oxygen packing can be drawn. Surprisingly, even after 1200 electrochemical cycles, only a very slight broadening of the XRD lines is observed. This behaviour results from the very small bond length modifications induced by the lithium de-intercalation and intercalation, even if changes in the unit cell symmetry occur [6,9]. This textural stability of the positive electrode material is particularly well emphasized by a comparative scanning electron microscopy study performed on these materials. The study of the surface of an electrode removed from the cell after 1200 cycles shows the simultaneous pres-

ence of agglomerates and single particules of $LiNiO_2$. One of these agglomerates is represented in Fig. 10(a) in comparison with that of an uncycled electrode (Fig. 10(b)). In Fig. 11, one can distinguish, at a higher magnification, the $LiNiO_2$ crystallites that constitute the agglomerates. They do not exhibit any visible size change, after (Fig. 11(a)) and before (Fig. 11(b)) cycling. The similarity between both pictures shows the textural stability of this material when lithium is de-intercalated and re-intercalated. This result, as well as the X-ray one, show clearly that there is no significant 'electrochemical grinding' of the $LiNiO_2$ crystallites during a long range battery cycling.

In order to detect modifications in the electrochemical behaviour resulting from cycling, lithium laboratory experimental cells have been built as described above, starting from the material cycled 5, 250 and 1200 times in a C/$LiNiO_2$ cell. These cells have been cycled at low rate (*C*/100) in the 4.15–3.0 V range; the cycling curves of the 5th and 1200th are reported in Fig. 12. They show a small decrease in capacity when the number of cycles previously performed increases. The cell polarization of materials cycled 5 and 250 times are almost similar; for those cycled 1200 times the low voltage part of the cycling curve resembles the other ones,

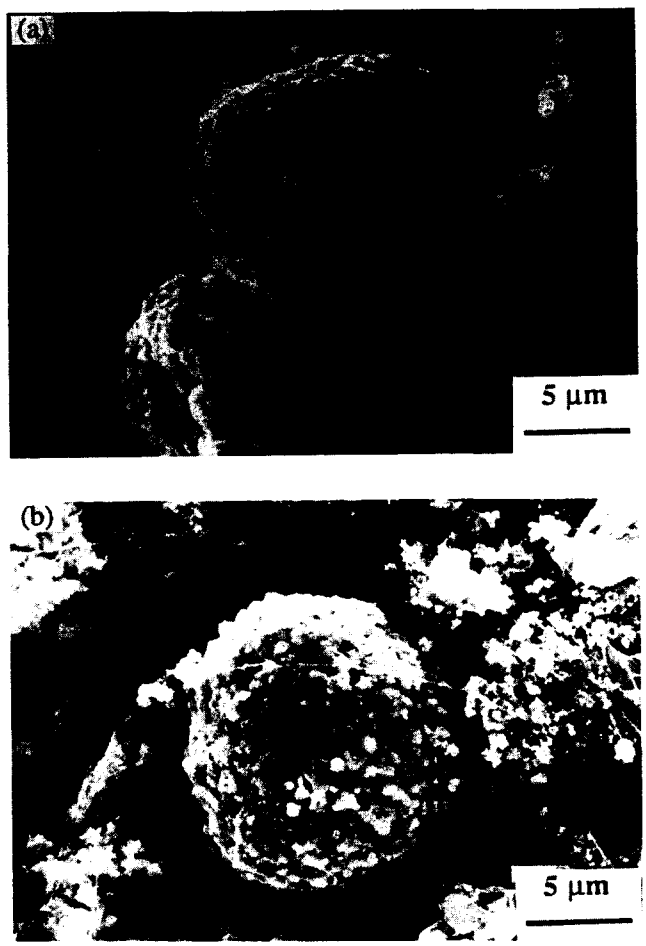

Fig. 10. Scanning electron microscopy of one agglomerate of $LiNiO_2$ (magnification ×4000; reduced in reproduction 88%): (a) removed from the cell after 1200 cycles, and (b) uncycled initial material.

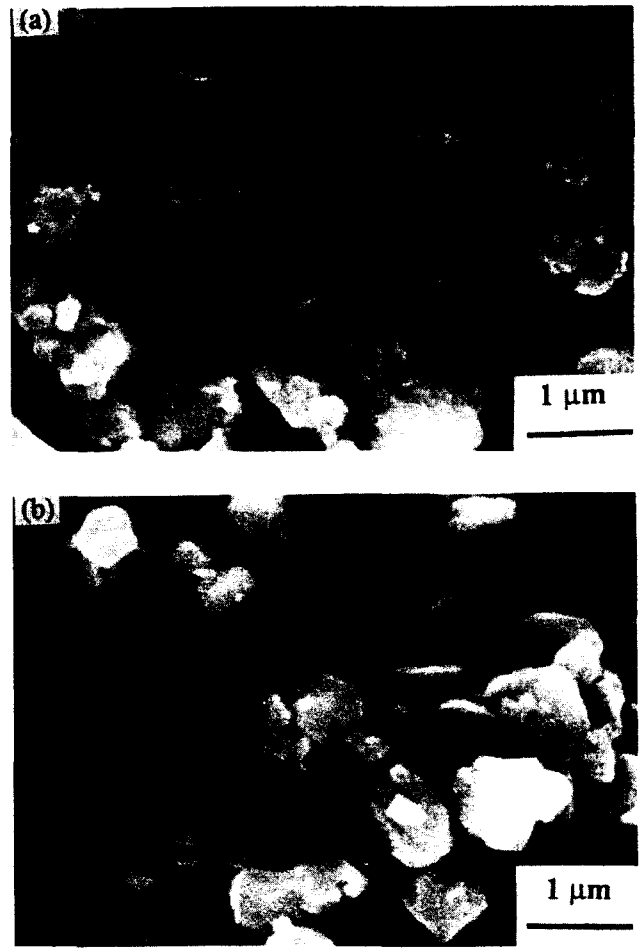

Fig. 11. Scanning electron microscopy of the $LiNiO_2$ crystallites (magnification ×20 000; reduced in reproduction 88%): (a) removed from the cell after 1200 cycles, and (b) uncycled initial material.

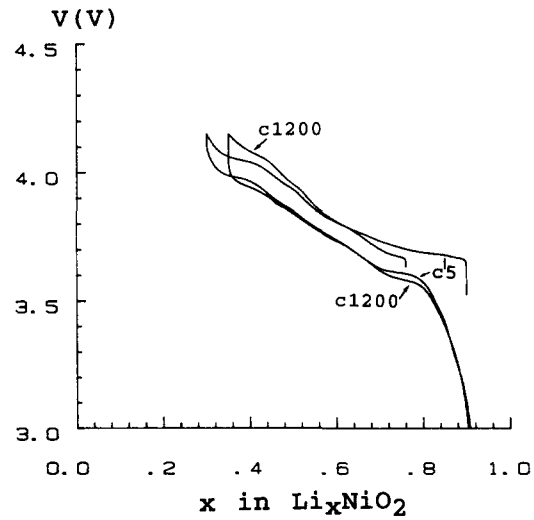

Fig. 12. Variations of Li/Li_xNiO_2 cell voltage vs. lithium amount using previously cycled materials: after 5 (c5) and 1200 cycles (c1200).

while the polarization significantly increases in the high voltage part.

5. Conclusions

$LiNiO_2$ is a very promising cathode material for rechargeable cells using a lithiated carbon anode. Preliminary results of prototypes indicate that the expected performances of commercial cells can be used in a lot of applications either portable or not, in different suitable design configurations. In addition, the cost reduction compared with cobalt-based material is particularly attractive.

Acknowledgements

The authors thank CNES, DRET and ADEME for financial support and C. Denage for the scanning electron microscopy study.

References

[1] A. Lecerf, M. Broussely and J.P. Gabano, *EP Patent No. 0 345 707; US Patent No. 4 980 080* (1989).

[2] M. Broussely, F. Perton, J. Labat, R.J. Staniewicz and A. Romero, *J. Power Sources, 43/44* (1993) 209–216.

[3] J. Morales, C. Perez-Vicente and J.L. Tirado, *Mater. Res. Bull., 25* (1990) 623.

[4] A. Rougier, P. Gravereau and C. Delmas, to be published.

[5] C. Delmas, I. Saadoune and A. Rougier, *J. Power Sources, 43/44* (1993) 595–602.

[6] T. Ohzuku, A. Ueda, M. Nagayama, Y. Ywakoshi and H. Komori, *Electrochim. Acta, 38* (1993) 1159–1167.

[7] J.R. Dahn, U. Von Sacken, M.W. Juzkow, H. Al-Janaby, *J. Electrochem. Soc., 138* (1991) 2207.

[8] J.R. Dahn, U. Von Sacken and C.A. Michal, *Solid State Ionics, 44* (1990) 87.

[9] W. Li, J.N. Reimers and J.R. Dahn, *Solid State Ionics, 67* (1993) 123.